JACS
JOURNAL OF THE AMERICAN CHEMICAL SOCIETY

COMMUNICATION

pubs.acs.org/JACS

New Microporous Metal−Organic Framework Demonstrating Unique Selectivity for Detection of High Explosives and Aromatic Compounds

Sanhita Pramanik,[†] Chong Zheng,[‡] Xiao Zhang,[†] Thomas J. Emge,[†] and Jing Li*[,†]

[†]Department of Chemistry and Chemical Biology, Rutgers, The State University of New Jersey, 610 Taylor Road, Piscataway, New Jersey 08852, United States

[‡]Department of Chemistry and Biochemistry, Northern Illinois University, DeKalb, Illinois 60115, United States

Supporting Information

ABSTRACT: A highly luminescent three-dimensional microporous metal−organic framework, $[Zn_2(oba)_2(bpy)]\cdot$DMA, demonstrates unique selectivity for the detection of high explosives and other aromatics via a fluorescence quenching and enhancement mechanism.

Rapid detection of explosives and explosive-like substances is a very important aspect concerning homeland security and environmental safety.[1] Current detection methods typically involve canines[2] or sophisticated instruments.[3] Both techniques are expensive and may not always be easily accessible. Fluorescence quenching employing conjugated polymers is a simple and promising alternative procedure that is based on the donor−acceptor electron-transfer mechanism.[4−7] Conjugated polymers are excellent electron donors, and their donor ability is enhanced by the delocalized π^* excited state, which facilitates exciton migration and hence increases the electrostatic interaction between the polymer and electron-deficient nitroaromatic analytes.[4,7,8]

Microporous metal−organic frameworks (MMOFs) are a new type of crystalline porous material that has shown strong potential for applications in gas storage and separation, catalysis, and sensing.[9] Very recently, we demonstrated that these materials are capable of very fast, fully reversible, and highly sensitive detection of high explosives such as 2,3-dimethyl-2,3-dinitrobutane (DMNB) and dinitrotoluene (DNT) in the vapor phase.[10] Herein we report a highly luminescent MMOF, $[Zn_2(oba)_2(bpy)]\cdot$DMA (**1**) [H_2oba = 4,4′-oxybis(benzoicacid); *bpy* = 4,4′-bipyridine; DMA = *N*,*N*′-dimethylacetamide], and its unique photoluminescence (PL) properties and high selectivity toward distinctively different groups of nitroaromatics and high explosives. The origin of such selectivity can be attributed to the electronic properties of both the MMOF and the analytes as well as the nature of their interactions in the excited states, on the basis of the results of molecular orbital (MO) and electronic band structure calculations as well as electrochemical (cyclic voltammetry) measurements.

Transparent cubic crystals of **1** were grown by solvothermal reactions. The structure of **1** was determined by single-crystal X-ray diffraction analysis [see Table S1 in the Supporting Information (SI)].[11] Compound **1** possesses a porous three-dimensional (3D) network built from a $Zn_2(oba)_4$ paddle-wheel secondary building unit (SBU). Each SBU is linked by *oba* to form a distorted 4^4 two-dimensional (2D) network. Two identical 4^4 nets interpenetrate to form a layered structure. The *bpy* acts as a linker between the paddle-wheel units from two adjacent layers to yield a highly stable 3D framework (Figure 1a−c). The structure contains one-dimensional (1D) open channels running along both the *a* and *b* axes, where the DMA molecules reside. The sizes and shapes of the channels were estimated by He simulation (Figure 1d).[12] The smallest cross sections of the two channels are ~5.8 Å × 8.3 Å. The solvent-accessible volume was calculated to be 25%. The structure remains intact upon removal of guest DMA molecules by heating at 160 °C (see the SI).

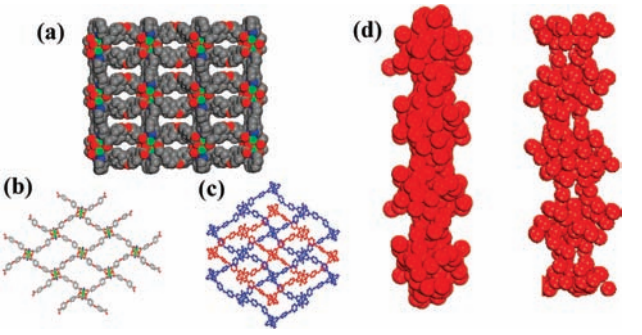

Figure 1. Crystal structure of **1**. (a) Space-filling model of the 3D framework, showing the 1D channels running along the *a* axis (DMA molecules have been removed for clarity). (b) A single 2D layer (Zn, green; O, red; N, blue). (c) Twofold interpenetration, shown by two different colors (blue and red). (d) He atom filling[12] in a single channel along the (left) *b* and (right) *a* axes.

PL spectra were recorded on powder samples of **1**′ (the guest-free form of **1**) in thin-layer form, and it was found that the compound emits strongly at 420 nm upon excitation at 280 nm (see the SI). The sensing and detection study was primarily focused on two different categories of aromatic compounds, namely, compounds containing electron-withdrawing groups such as nitroaromatics (group A) and those having electron-donating groups such as CH_3 (group B).

We found that all nitroaromatics act as fluorescence quenchers for **1**′. Among them, the most effective quencher is nitrobenzene (NB) and the least effective one is DNT. The quenching efficiency (%) was estimated using the formula $(I_0 - I)/I_0 \times 100\%$, where I_0 is the maximum fluorescence intensity of **1**′ before exposure to the analyte. NB quenches the emission by as

Received: July 31, 2010
Published: March 08, 2011

dx.doi.org/10.1021/ja106851d | *J. Am. Chem. Soc.* 2011, 133, 4153–4155

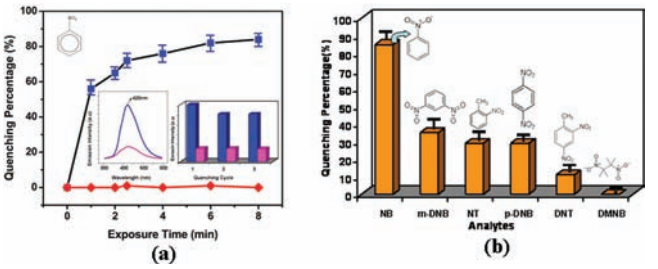

Figure 2. (a) Time-dependent fluorescence quenching by NB (blue ■) and DMNB (red ◆). Insets: (left) corresponding emission spectra before and after exposure of **1′** to the NB vapor; (right) results for three continuous quenching cycles. (b) Percentage of fluorescence quenching after 15 min by five different analytes from group A at room temperature.

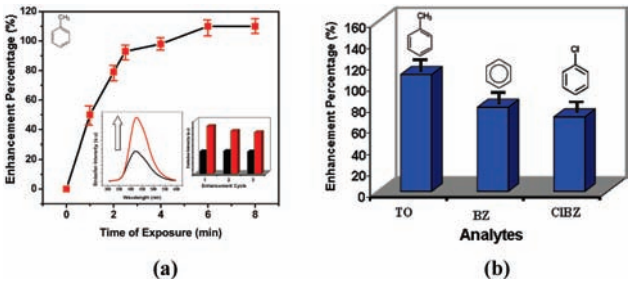

Figure 3. (a) Time-dependent fluorescence enhancement of TO. Insets: (left) corresponding emission spectra before and after exposure of **1′** to TO vapors for 15 min; (right) results for three consecutive quenching cycles. (b) Percentage of fluorescence enhancement by three group-B analytes at room temperature.

much as 84% (Figure 2a), and the order of quenching efficiency for the selected nitroaromatics is NB > *m*-DNB > NT ≈ *p*-DNB > DNT (Figure 2b; NT, nitrotoluene; DNB, dinitrobenzene). Notably, this order is not fully in accordance with the trend of electron-withdrawing groups, but it is fully consistent when the vapor pressure of each analyte is also taken into consideration. The fact that NB exhibits the strongest quenching effect can be attributed to two factors: the high vapor pressure and the strongly electron-withdrawing $-NO_2$ group (see Table S2). Although the vapor pressure of NT is comparable to that of NB, the quenching efficiency (29%) is significantly less because of the presence of the electron-donating $-CH_3$ group. Similarly, while *m*- and *p*-DNB have two strongly electron-withdrawing $-NO_2$ groups, both have very low vapor pressures at room temperature (see Tables S2 and S5). In all cases, **1′** could be fully regenerated simply by heating it at 150 °C for a few minutes after each measurement (Figures 2a and 3a, far-right insets).

An opposite effect was observed for group-B analytes. Unlike group-A nitroaramatics, these non-nitro-containing aromatics appeared to enhance the luminescence emission of **1′**. Toluene (TO) enhanced the emission intensity most significantly (by 120%), followed by benzene (BZ) and chlorobenzene (ClBZ). The observed trend (Figure 3b) is fully consistent with their electron-donating abilities and vapor pressures.

The observed fluorescence attenuation and enhancement can be explained by the donor−acceptor electron-transfer mechanism. In the case of a group-A aromatic analyte, the lowest unoccupied MO (LUMO) is a low-lying π^*-type orbital stabilized by the NO_2 group through conjugation (see Figure S20 in the SI), and its energy is below the conduction band (CB)

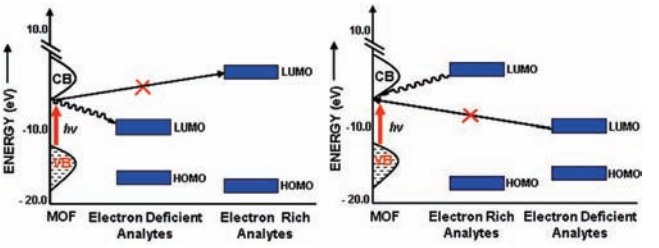

Figure 4. Schematic drawings of the electronic structure of (left) the fluorescence quenching process by a group-A aromatic analyte having an electron-withdrawing functional group and (right) the fluorescence enhancment process by a group-B aromatic analyte having an electron-donating functional group. See the SI for details of the MO and band structure calculations.

of **1′**. Although all MOFs have extended network structures, they are often characterized by narrow energy bands because of highly localized electronic states, especially those containing d^{10} metals. In such cases, they may be regarded as giant "molecules", and their valence band (VB) and CB energy levels can be described in a way similar to that for MOs.

Upon excitation, electrons are transferred from the CB of **1′** to the LUMO of the analyte, leading to a quenching effect (Figure 4a). This mechanism has been well-developed for conjugated polymers[4,6,7a,13] and was confirmed here for **1′** on the basis of our MO and band structure calculations (see the SI). For an aromatic analyte from group B, the excited electrons from its LUMO, a high-lying π^* antibonding state with its energy above the CB of the MMOF, are transferred to the CB of **1′**, thereby leading to fluorescence enhancement (Figure 4b). Alternatively, the electron transfer between the photoexcited state of **1′** and the analyte may be assessed by their reduction potentials.[14] Our cyclic voltammetry measurements showed that group-A analytes have reduction potentials more positive than that of **1′**, while those of group-B analytes are more negative (see Table S6). Therefore, **1′** acts as an electron donor in the case of group-A analytes and an electron acceptor in the case of group-B analytes. It should be pointed out that while the two descriptions/mechanisms are consistent and both are based on the relative orbital energy levels of the MMOF and analyte, more in-depth studies are required in order to fully understand the origin of the quenching/enhancement effect.

On the other hand, DMNB shows a negligible quenching effect in **1′** (<1%; see Figure 2a). This is very different from the behavior of $Zn_2(bpdc)_2(bpee)$ reported earlier,[10] for which DNT and DMNB gave very similar quenching profiles (maxima at ∼84−85%). This distinctly dissimilar behavior makes **1′** an excellent candidate for selective detection of high explosives from different categories. The difference is most likely due to the following reasons: First, the size of the pores in **1′** (∼7.1 Å × 7.3 Å × 7.7 Å; see Table S3) is too small for a nonplanar, bulky DMNB molecule to enter. Second, the orbital overlap between this type of analyte (aliphatic nitro-containing molecules) and the MMOF is very weak. Third, the reduction potentials of DMNB and **1′** are similar (see Table S6), suggesting that the two species have comparable reduction capabilities and therefore that a driving force for electron transfer between the two is lacking. To verify and further understand the cause of this phenomenon, we investigated the fluorescence behavior of **1′** upon exposure to smaller nitro-containing analytes, including nitromethane (NM), nitroethane (NE), and 1-nitropropane (1-NP). These molecules

dx.doi.org/10.1021/ja106851d |*J. Am. Chem. Soc.* 2011, 133, 4153–4155

are sufficiently small that they can enter the pores in **1′** without any difficulty. The results showed that they also have no effect on the PL properties of **1′**, very much the same as DMNB (see Figure S14). The measured reduction potentials are in the same range as that of DMNB, demonstrating that they too have reduction capabilities similar to that of **1′**. Band structure calculations also showed that the extent of LUMO−CB interaction is very different for the two groups. The orbital overlap between the LUMO of nitrobenzene (a nitro-containing aromatic analyte) and the conduction band of **1′** was calculated to be 0.27, indicative of a strong interaction, whereas the overlap between the LUMO of nitromethane (a nitro-containing nonaromatic analyte) and the conduction band of **1′** is only 0.05, indicating a very weak interaction. This is because the π-type orbital of an aromatic analyte overlaps much better with the π-type conduction band of **1′** than the σ-type LUMO of a nonaromatic analyte (see Figures S15, S20, and S21).

In summary, a highly luminescent microporous metal−organic framework, $[Zn_2(oba)_2(bpy)]\cdot$DMA (**1**), illustrates unprecedented sensing and detection properties. Our studies on its guest-free form, **1′**, revealed unique fluorescence quenching and enhancement behavior upon exposure to the vapor of aromatic compounds of group A (having electron-withdrawing groups) and group B (having electron-donating groups), respectively. These studies also showed that nitro-containing nonaromatic analytes have a negligible effect on the fluorescence of the MMOF. The results demonstrate the exceptional ability of **1′** to selectively detect explosives of different types (e.g., aromatic DNT vs nonaromatic or aliphatic DMNB). The origin of such an effect can be understood and explained on the basis of MO and band structure calculations as well as a comparison of their electrochemical properties. Clearly, the nature of the analyte molecules and the electronic structure and porosity of the MMOF all play key roles in the emission properties. The work represents the very first example of the MMOF family that exhibits such phenomena.

■ ASSOCIATED CONTENT

Supporting Information. Synthesis and selected crystallographic data (CIF) of **1**; PXRD, TGA, and PL experimental procedures; calculation details; and additional figures. This material is available free of charge via the Internet at http://pubs.acs.org.

■ AUTHOR INFORMATION

Corresponding Author
jingli@rutgers.edu

■ ACKNOWLEDGMENT

The authors acknowledge the National Science Foundation for its generous support of this work through Grant DMR-0706069.

■ REFERENCES

(1) Smith, K. D.; McCord, B. R.; McCrehan, W. A.; Mount, K.; Rowe, W. F. *J. Forensic Sci.* **1999**, *44*, 789.
(2) Czarnik, A. W. *Nature* **1998**, *398*, 417.
(3) Moore, D. S. *Rev. Sci. Instrum.* **2004**, *75*, 2499.
(4) Toal, S. J.; Trogler, W. C. *J. Mater. Chem.* **2006**, *16*, 2871.
(5) (a) Rose, A.; Zhu, Z.; Madigan, C. F.; Swager, T. M.; Bulovic, V. *Nature* **2005**, *434*, 876. (b) McQuade, D. T.; Pullen, A. E.; Swager, T. M. *Chem. Rev.* **2000**, *100*, 2537.
(6) Thomas, S. W., III; Joly, G. D.; Swager, T. M. *Chem. Rev.* **2007**, *107*, 1339.
(7) (a) Yang, J.-S.; Swager, T. M. *J. Am. Chem. Soc.* **1998**, *120*, 11864. (b) Yang, J.-S.; Swager, T. M. *J. Am. Chem. Soc.* **1998**, *120*, 5321.
(8) Swager, T. M. *Acc. Chem. Res.* **1998**, *31*, 201.
(9) (a) Férey, G. *Chem. Soc. Rev.* **2008**, *37*, 191. (b) Yaghi, O. M. *Nat. Mater.* **2007**, *6*, 92. (c) Pan, L.; Parker, B.; Huang, X.; Olson, D. H.; Lee, J.; Li, J. *J. Am. Chem. Soc.* **2006**, *128*, 4180. (d) Pan, L.; Liu, H.; Lei, X.; Huang, X.; Olson, D. H.; Turro, N.; Li, J. *Angew. Chem., Int. Ed.* **2003**, *42*, 542. (e) Murray, L. J; Dincă, M.; Long, J. R. *Chem. Soc. Rev.* **2009**, *38*, 1294. (f) Lee, J. Y.; Farha, O. K.; Roberts, J.; Scheidt, K. A.; Nguyen, S. T.; Hupp, J. T. *Chem. Soc. Rev.* **2009**, *38*, 1450.
(10) Lan, A.; Li, K.; Wu, H.; Olson, D. H.; Emge, T. J.; Ki, W.; Hong, M.; Li, J. *Angew. Chem., Int. Ed.* **2009**, *48*, 2334.
(11) Crystal data for **1**: $C_{42}H_{33}N_3O_{11}Zn$, M = 886.45 g/mol; orthorhombic, space group *Pcca*; a = 16.838(3) Å, b = 11.026(2) Å, c = 22.410(5) Å; V = 4160.5(14) Å^3; Z = 4; $F(000)$ = 4078; D_{calcd} = 1.415 g cm^{-3}; μ(Mo Kα) = 1.215 mm^{-1}; T = 293(2) K; R_1 = 0.0626, wR_2 = 0.1835 with $I \geq 2\sigma(I)$; GOF = 1.065.
(12) Cerius^2 3.0 Molecular Simulation Package.
(13) (a) Toal, S. J.; Sanchez, J. C.; Dugan, R. E.; Trogler, W. C. *J. Forensic Sci.* **2007**, *52*, 79. (b) Sohn, H.; Sailor, M. J.; Magde, D.; Trogler, W. C. *J. Am. Chem. Soc.* **2003**, *125*, 3821.
(14) *Photophysics of Organometallics*; Lees, A. J., Ed.; Topics in Organometallic Chemistry, Vol. 29; Springer: New York, 2010.